

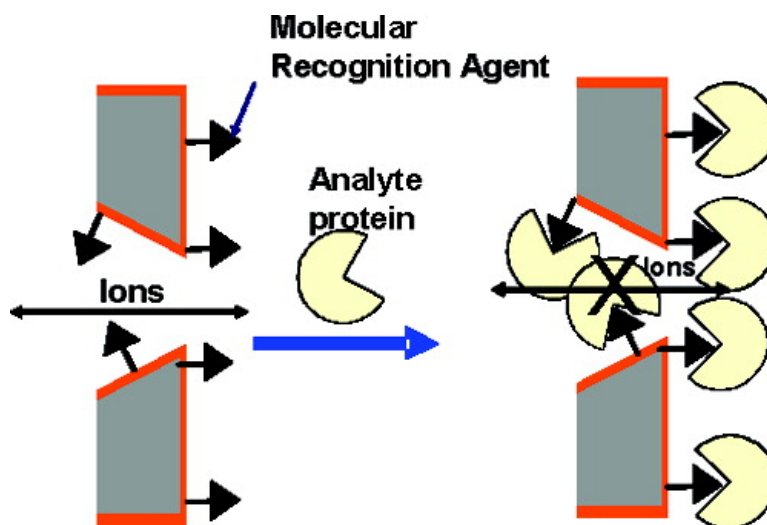
Communication

**Protein Biosensors Based on Biofunctionalized Conical Gold Nanotubes**

Zuzanna Siwy, Lacramioara Trofin, Punit Kohli, Lane A. Baker, Christina Trautmann, and Charles R. Martin

*J. Am. Chem. Soc.*, **2005**, 127 (14), 5000-5001 • DOI: 10.1021/ja043910f • Publication Date (Web): 15 March 2005

Downloaded from <http://pubs.acs.org> on March 25, 2009



**More About This Article**

Additional resources and features associated with this article are available within the HTML version:

- Supporting Information
- Links to the 17 articles that cite this article, as of the time of this article download
- Access to high resolution figures
- Links to articles and content related to this article
- Copyright permission to reproduce figures and/or text from this article

[View the Full Text HTML](#)

## Protein Biosensors Based on Biofunctionalized Conical Gold Nanotubes

Zuzanna Siwy,<sup>†</sup> Lacramioara Trofin,<sup>†</sup> Punit Kohli,<sup>†</sup> Lane A. Baker,<sup>†</sup> Christina Trautmann,<sup>‡</sup> and Charles R. Martin<sup>\*†</sup>

Department of Chemistry and Center for Research at the Bio/Nano Interface, University of Florida, Gainesville, Florida 32611-7200, and GSI Darmstadt, Planckstrasse 1, 64291 Darmstadt, Germany

Received October 6, 2004; E-mail: crmartin@chem.ufl.edu

There is increasing interest in using nanopores as the sensing elements in biosensors.<sup>1,2</sup> The nanopore most often used is the  $\alpha$ -hemolysin protein channel, and the sensor consists of a single channel embedded within a lipid bilayer membrane. An ionic current is passed through the channel, and analyte species are detected as transient blocks in this current associated with translocation of the analyte through the channel—stochastic sensing.<sup>1</sup> While this is a very promising sensing paradigm, it would be advantageous to eliminate the fragile lipid bilayer membrane and perhaps to replace the biological nanopore with an abiotic equivalent.<sup>2</sup>

We describe here a new type of protein biosensor that is based on a single conically shaped gold nanotube embedded within a mechanical and chemically robust polymeric membrane. The sensing protocol also entails passing an ionic current through the nanotube, but unlike the previous devices,<sup>1,2</sup> transient current pulses are not observed and analyzed. Instead, the protein analyte binds to a biochemical molecular-recognition agent immobilized at the small diameter opening (or mouth) of the conical nanotube. Because the protein molecule and the nanotube mouth have comparable diameters, analyte binding effectively plugs the nanotube, which is detected as a corresponding permanent blockage of the ion current.

Single conically shaped nanopores were etched into  $\sim 0.8$  cm<sup>2</sup> samples of a 12- $\mu$ m-thick poly(ethylene terephthalate) membrane.<sup>3</sup> The large diameter opening at one face of the membrane was  $\sim 600$  nm, and the small diameter opening at the opposite face was  $\sim 30$  nm. Electroless gold plating was used to deposit a conical Au nanotube along the walls of this pore; both faces of the membrane are also coated with Au.<sup>4</sup> Because the Au layer deposited is so thin, the large diameter opening of the conical Au nanotube remained  $\sim 600$  nm. The mouth diameter was controlled by varying the electroless plating time<sup>4</sup> and measured using a simple electrochemical method.<sup>3,5</sup> Au nanotubes with mouth diameters in the range of 5–9 nm were used, depending on the analyte to be detected.<sup>5</sup>

The final step was to attach the molecular-recognition agent (MRA) to the Au surfaces.<sup>5</sup> Three different MRA/analyte systems were investigated: biotin/streptavidin,<sup>6</sup> protein-G/immunoglobulin (IgG),<sup>7</sup> and an antibody to the protein ricin<sup>8</sup> as the MRA and ricin as the analyte. Biotin was attached to the Au by using a commercial thiolated biotin derivative.<sup>5</sup> A commercial biotinylated protein G was used for the IgG sensor. The Au nanotube was first biotinylated, streptavidin (SA) was then attached to the surface-bound biotin, and the biotinylated protein G was attached to the SA.<sup>5</sup> A similar strategy was used to attach biotinylated anti-ricin.<sup>5</sup> The nanotube mouth diameter was remeasured after each of the functionalized steps.<sup>5</sup> The final mouth diameters (after all functionalization steps) were SA sensor and IgG sensor  $\sim 5$  nm, ricin sensor  $\sim 4$  nm.<sup>5</sup>

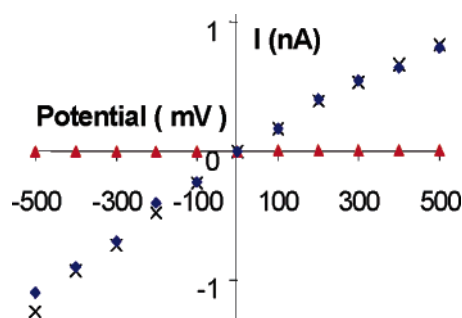


**Figure 1.**  $I$ – $V$  curves for the SA sensor in the presence of no protein ( $\times$ ), 100 nM lysozyme ( $\blacklozenge$ ), and 180 pM SA ( $\blacktriangle$ ).

The membrane sample was mounted between the two halves of a conductivity cell,<sup>3</sup> and each half-cell was filled with  $\sim 1.7$  mL of a 1 M phosphate buffer solution (pH = 4.5 for IgG and ricin, pH = 9 for SA) that was also 1 M in KCl. A Ag/AgCl electrode was inserted into each half-cell solution, and an Axopatch 200B (Axon Instruments) was used to apply the desired transmembrane potential and measure the resulting ion current flowing through the nanotube.<sup>3</sup> The measurement procedure was as follows: 1. Obtain a current–voltage ( $I$ – $V$ ) curve before exposure to protein. 2. Replace the solution facing the mouth of the nanotube with an electrolyte solution of a protein that *does not bind* to the attached MRA and obtain a second  $I$ – $V$  curve. 3. Replace this solution with a solution of the protein that *does bind* to the MRA and obtain the  $I$ – $V$  curve.

Because biotin binds SA with high affinity and selectivity, the biotin/SA system is often used as a test case for biosensor development.<sup>6a</sup>  $I$ – $V$  curves for the biotinylated nanotube before and after exposure to a solution that was 100 nM in lysozyme are identical (Figure 1), indicating that the sensor does not respond to a protein that *does not bind* to the biotin MRA. Identical results were obtained for the nonbinding protein bovine serum albumin (BSA).<sup>5</sup> In contrast, the ion current is completely shut off (the residual current is within the noise level of the potentiostat)<sup>5</sup> after exposure to a solution that was 180 pM in the analyte protein SA (Figure 1). Total blockage occurs because the diameter of the SA molecule,  $\sim 5$  nm,<sup>6b</sup> is comparable to the mouth diameter for the biotinylated nanotube.

Because the number of SA molecules that encounter the membrane surface per second decreases with SA concentration, the time required for blockage,  $\tau_b$ , is inversely related to concentration (Figure 2);  $\tau_b$  can, therefore, be used to determine the analyte concentration. While the  $\tau_b$  values for the lowest concentrations are long,  $\tau_b$  can be shortened by convectively transporting the analyte to the nanotube mouth.<sup>9</sup> For charged analytes, electrophoresis provides a powerful way to apply convective transport.<sup>9,10</sup> Indeed, Lee et al. have shown that the time required to drive charged particles to the mouth of a nanopore can be controlled at will in this way.<sup>9</sup> The error in  $\tau_b$  also increases with decreasing [SA]

<sup>†</sup> University of Florida.

<sup>‡</sup> GSI Darmstadt.

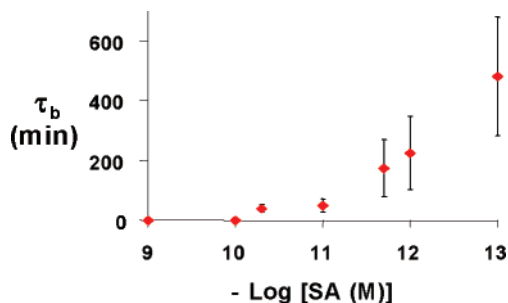


**Figure 2.** Blockage time vs  $-\log$  of the molar SA concentration. The error bars are associated with three replicate measurements done with three different identical nanotube sensors.

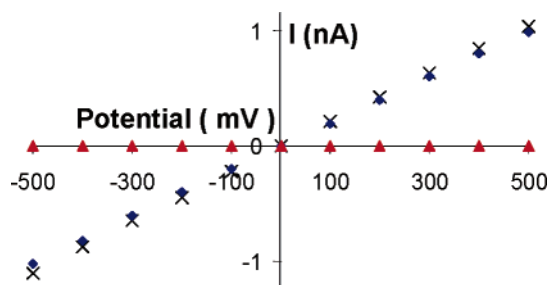


**Figure 3.**  $I$ – $V$  curves for the horse IgG sensor in the presence of no protein ( $\times$ ), 10 nM cat IgG ( $\blacklozenge$ ), and 10 nM horse IgG ( $\blacktriangle$ ).

(Figure 2). However, since  $\tau_b$  can be decreased by electrophoretically driving the analyte to the nanotube,<sup>9</sup> and since the error in  $\tau_b$  is less for smaller  $\tau_b$  values, it should be possible to obtain better reproducibility at low concentrations if convective transport is used.

The second sensor uses protein G<sup>7</sup> as the MRA. Protein G binds IgG, but the binding affinity depends on the species from which the IgG was derived; for example, protein G binds strongly to horse IgG but not to cat IgG.<sup>7</sup> Hence, horse IgG can act as the analyte, and cat IgG as the nonbinding control. As expected, cat IgG has no effect on the  $I$ – $V$  curve for this sensor, whereas horse IgG blocks the nanotube and shuts off the ion current (Figure 3). We have shown that such blockage occurs for analyte horse IgG concentrations in the 100–10 nM range, but lower concentrations have not yet been investigated.

Because IgGs are very flexible molecules,<sup>11a</sup> it is more difficult to correlate the size of the analyte (IgG) with the diameter of the nanotube mouth. However, protein G binds to the Fc part of the IgG molecule,<sup>11b</sup> and the diameter of this fragment, 4 nm,<sup>11a</sup> is comparable to the mouth diameter of the functionalized nanotube.

Ricin<sup>8</sup> (molecular weight = 60 kDa) is a highly toxic protein and has been used as bioterror agent. However, the protein that we used<sup>5</sup> had <1% of the toxicity of the wild-type protein. Exposure of the anti-ricin-based sensor to ricin shuts down the ion current, whereas exposure to nonbinding BSA has no effect on the  $I$ – $V$  curve (Figure 4).

We have demonstrated a new class of highly sensitive and selective protein biosensors based on biofunctionalized conical Au nanotubes. This sensing paradigm is similar to stochastic sensing;<sup>1,2</sup> however, detection is not based on measurement of transient current pulses. Indeed, it should be possible to simply hold the transmembrane potential constant and detect analyte by a drop in the steady-

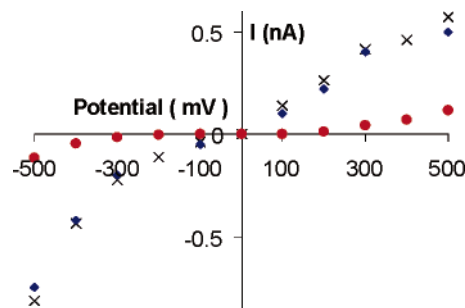


**Figure 4.**  $I$ – $V$  curves for the ricin sensor in the presence of no protein ( $\times$ ), 100 nM BSA ( $\blacklozenge$ ), and  $\sim$ 100 nM ricin ( $\bullet$ ).

state ion current. That is, one should be able to operate these devices like a household smoke detector. The use of a mechanically and chemically stable membrane and nanotube is another attractive feature of these new biosensors. Furthermore, with the strong-binding MRAs used here, these sensors are essentially “one-use” devices. However, if a weaker binding MRA is used, the sensors could be rejuvenated and used multiple times.

Finally, while it may be possible to make analogous devices using cylindrical nanotubes or pores, the conical geometry has the following advantages: 1. For any mouth diameter, the ion current in a conical nanotube/pore can be orders of magnitude higher than that in a cylindrical tube/pore of the same diameter.<sup>5</sup> 2. The conical tube/pore is less susceptible to unwanted plugging. 3. The voltage drop in a conical tube/pore is focused to the mouth,<sup>9</sup> making the conical geometry ideally suited for detecting analyte binding there.

**Acknowledgment.** This work was supported by the National Science Foundation.

**Supporting Information Available:** Details of preparation and biofunctionalization of the nanotubes. This material is available free of charge via the Internet at <http://pubs.acs.org>.

## References

- (1) (a) Kasianowicz, J. J.; Brandin, E.; Branton, D.; Deamer, D. W. *Proc. Natl. Acad. Sci. U.S.A.* **1996**, *96*, 13770–13773. (b) Bayley, H.; Cremer, P. S. *Nature* **2001**, *413*, 226–230. (c) Henriquez, R. R.; Ito, T.; Sun, L.; Crooks, R. M. *Analyst* **2004**, *129*, 478–482. (d) Deamer, D. W.; Branton, D. *Acc. Chem. Res.* **2002**, *35*, 817.
- (2) (a) Li, J.; Stein, D.; McMullan, C.; Branton, D.; Aziz, M. J.; Golovchenko, J. A. *Nature* **2001**, *412*, 166–169. (b) Saleh, O. A.; Sohn, L. L. *Nano Lett.* **2003**, *3*, 37–38. (c) Mara, A.; Siwy, Z.; Trautmann, C.; Wan, J.; Kamme, F. *Nano Lett.* **2004**, *4*, 497–501. (d) Li, J.; Gershow, M.; Stein, D.; Brandin, E.; Golovchenko, J. A. *Nat. Mater.* **2003**, *2*, 611–615.
- (3) Apel, P.; Korchev, Y. E.; Siwy, Z.; Spohr, R.; Yoshida, M. *Nucl. Instrum. Methods B* **2001**, *184*, 337–346.
- (4) Martin, C. R.; Nishizawa, M.; Jirage, K. B.; Kang, M. J. *Phys. Chem. B* **2001**, *105*, 1925–1934.
- (5) See Supporting Information for details.
- (6) (a) Movileanu, L.; Howorka, S.; Braha, O.; Bayley, H. *Nat. Biotechnol.* **2000**, *18*, 1091–1095. (b) Hendrickson, W. A.; Pahler, A.; Smith, J. L.; Satow, Y.; Merritt, E. A.; Phizackerly, R. P. *Proc. Natl. Acad. Sci. U.S.A.* **1989**, *86*, 2190–2194.
- (7) Bjorck, L.; Kronvall, G. *J. Immunol.* **1984**, *133*, 969–972.
- (8) Poli, M. A.; Rivera, V. R.; Hewetson, J. F.; Merrill, G. A. *Toxicon* **1994**, *32*, 1371–1377.
- (9) Lee, S.; Zhang, Y.; White, H. S.; Harrell, C. C.; Martin, C. R. *Anal. Chem.* **2004**, *76*, 6108–6115.
- (10) Yu, S.; Lee, S. B.; Martin, C. R. *Anal. Chem.* **2003**, *75*, 1239–1244.
- (11) (a) Zhou, D.; Wang, X.; Birch, L.; Rayment, T.; Abell, C. *Langmuir* **2003**, *19*, 10557–10562. (b) Akerstrom, B.; Brodin, T.; Reis, K.; Bjorck, L. *J. Immunol.* **1985**, *135*, 2589–2592.

JA043910F